ELSEVIER

International Journal of Heat and Fluid Flow 21 (2000) 104–111

International Journal of HEAT AND FLUID FLOW

www.elsevier.com/locate/ijhff

Measurement and simulation of pressure wave attenuation in upward air–water bubbly flow

H. Wang [a,*], G.H. Priestman [b], S.B.M. Beck [c], R.F. Boucher [d]

[a] *Department of Chemical and Materials Engineering, University of Alberta, Edmonton AB, Canada T6G 2G6*
[b] *Department of Chemical and Process Engineering, University of Sheffield, Sheffield, UK*
[c] *Department of Mechanical Engineering, University of Sheffield, Sheffield, UK*
[d] *UMIST, Manchester, UK*

Received 27 September 1997; accepted 17 June 1999

Abstract

This paper is concerned with the measurement and modelling of pressure wave transmission and attenuation in an upward air–water bubbly pipe flow. The pressure waves in this two phase mixture are produced by a fluidic pressure pulse transmitting flowmeter placed upstream of the vertical section. The pressure pulses produced by the flowmeter are proportional to the flow going through the flowmeter. This device has been shown to work well in single phase liquids, but it is known that oil production is predominately two phase (oil and gas). To this end, the attenuation of pressure pulses in two phase flow was a vital element in assessing the viability of this device. Experimental work has been conducted to do with measuring the attenuation of the pressure waves as they travel up a 6.6 m high, 0.1 m diameter vertical pipe, initially filled with water. Frequencies between 4 and 12 Hz and air void fractions up to 25% were used for this series of experiments. The average air bubble radius was measured as being 3 mm. High speed photography was employed to obtain a clear observation of the wave effect on the air bubbles. Theoretical modelling was conducted using a CFD package (FLUENT) in order to predict the wave decay in the bubbly flow. The modelled results were found to agree well with experimental measurement of signal attenuation, confirming the potential of the flowmeter for remote flow measurement of two phase bubbly flow.

Keywords: Pressure wave attenuation; Air–water bubbly flow; Bubble behaviour; CFD modelling; Flow measurement

1. Introduction

Modelling and measuring travelling pressure wave attenuation in pipe fluids is important in relation to oil production metering and information transmission in oil production strings. Two kinds of new flowmeter have been specially developed for remote oil flow measurement in oil production strings (Boucher et al., 1996; Wang et al., 1996, 1997, 1998). The proposed flowmeters produce downhole pressure pulses which are transmitted by wave action through the oil and oil–gas bubbly flow, respectively, in the pipe, to the surface for detection and recording. The application of such meters depends upon successful transmission of the pressure wave signal along the pipe fluids.

In the case of air flowing through pipes, the theoretical and experimental results of pressure wave attenuation were found to give good agreement (Wang et al., 1999). However, in two-phase bubbly flow, the mechanism of pressure wave transmission is far more complicated, and the wave attenuation is greater than in the single phase. Since it is difficult to model crude oil–gas bubbly flow in the laboratory, the pressure wave attenuation measurements have been conducted up a vertical pipe containing water with air bubbles. The measured results can be then compared to the results from theoretical modelling to enable prediction of the signal decay in an oil-gas two-phase bubbly flow.

The flow of the air–water bubbly mixture in a pipe is a complex phenomenon. The turbulent structure of an air–water bubbly upflow in a circular pipe has been investigated experimentally by many researchers e.g., Serizawa et al. (1975); Theofanous and Sullivan (1982); Liu and Bankoff (1993); Bertodano et al. (1994). Up to date, no complete mathematical model of the two phase flow has been derived. Some attempts e.g., Pauchon and Banerjee (1988); Lisseter and Fowler (1992); Vreenegoor and Geurst (1993), only predict the distribution of the air void fractions over a cross-section of the pipe for the two-phase bubbly flow. An experimental investigation of the pressure fluctuations due to bubble deformation was conducted by Leutheusser (1978). The propagation of interfacial pressure and void fraction fluctuation is another characteristic phenomenon of bubbly two-phase flow (Akselrod, 1993; Revankar and Ishii, 1992). Although wave phenomena in

* Corresponding author.
E-mail address: huahui.wang@ualberta.ca (H. Wang).

0142-727X/00/$ - see front matter
PII: S0142-727X(99)00052-1

bubbly liquid have been investigated by many researchers over the years (Silberman, 1957; Prosperetti and Kim, 1988; Commander and Prosperetti, 1989; Nigmatulin, 1982; Nakoryakov et al., 1990; Miksis and Ting, 1992; Chung et al., 1992; Kytomaa and Brennen, 1991; Beylich, 1994; Van Wijngaarden, 1995), including some recent development (Kameda and Matsumoto, 1996; Kameda et al., 1998), current understanding of the various wave disturbances in bubbly liquid is not satisfactory.

The new fluidic flowmeters (Wang et al., 1996, 1998), produce periodic variations in pressure downstream of the flowmeters. These pressure fluctuations can be regarded as severe pressure pulsations in the fluid down the pipe. In transient analysis of the pipe flow, these fluctuations may be expressed as harmonic pressure pulsating waves, which coincide with severe flow pulsations, or flow steady-oscillations. These waves can be also regarded as dynamic waves (Wallis, 1969), which propagate with the speed of sound through the fluid flow (Beck et al., 1995), the speed of sound depends on the type and temperature of the fluids (Thorley, 1991). Transmitting these waves is a forced oscillatory motion process, similar to the water hammer effect (Wylie and Streeter, 1985).

Travelling wave attenuation is a process during which some of the incident acoustic energy is converted to heat and some to new sound waves, which are out of phase with the incident wave. The attenuation of any pressure disturbance in the air–water bubbly flow is far higher than single phase flow. The presence of air bubbles has two effects on the acoustic properties of the mixture. Firstly the compressibility of the mixture increases. This will decrease the speed of sound of the mixture since the propagation sound velocity is inversely proportional to the square root of the mixture's compressibility. Secondly there is the additional acoustic energy absorption due to the bubbles themselves. Another important aspect of the two phase flow which is introduced along with the presence of the bubbles is that the applied wave frequency causes bubble oscillation. This can be very important when the wave frequency lies close to the bubble resonant frequency. Resonance causes a large radial displacement. The result is an increase of the attenuation constant and compressibility and therefore a reduction in the amplitude and the speed of the waves.

In general, the air–water bubbly fluid is a dispersive and dissipative medium, and the propagation properties of pressure waves depend on the air void fraction, size of the bubbles, amplitude of waves and frequency content of the imposed signals. Much research concerned with wave transmission in liquid–gas bubbly flow has been conducted by different researchers over the years (Hsieh and Plasset, 1961; Van Wijngaarden, 1972; Kuznestov et al., 1978; Ruggle, 1988; Watanabe and Prosperetti, 1994), producing different results which were based on different versions of the conservation equations from the Navier–Stokes equations. However, these results have little usage to the authors' present work. Furthermore the computer code of SUNAS, which comes from the authors' previous work (Beck and Boucher, 1993), treats the bubbly mixture as a non-Newtonian fluid and takes into account a two-phase flow parameter in modelling the wave attenuation, but this code requires refinement to handle the bubbly flow.

This paper describes the measurement and simulation of the transmission decay of forced pressure waves, as measured in a vertical flow rig operated with an upward air–water bubbly flow. High speed photography is used for detailed visual observation of the behaviour of air bubbles in a pressure wave. A CFD code, FLUENT, is also used to study the pressure wave decay in the upward bubbly pipe flow.

2. Experimental arrangement

The basic rig design is shown in Fig. 1. The original air–water loop consisted of a triplex piston pump, pressure wave generator (the brass BV pulse transmitting flowmeter (Wang et al., 1996)), bubble generator, test section, water header tank and a downcomer pipe. The flow was circulated by a triplex pumping unit. The water flow was controlled by a variable speed motor and measured by an electromagnetic flowmeter. The discharge of the triplex piston pump was limited to 100 l/min, although it could deliver a high pressure up to 10 MPa. To get a higher water flow, a centrifugal water pump was used in parallel as shown. The BV flowmeter generates the AC part of the pulsation in the flow and the centrifugal and the triplex piston pumps produce the DC part of the flow.

There was an air bubble generator placed at the bottom of the test section, which was supplied from a compressed air supply. Air bubbles were injected to the settled water flow around the bubble generator. Thus air–water bubble flow entered the pipe test section. Fig. 1 also shows the four elevations (P0, P1, P2, P3) of the measurement stations. Each of the stations was attached to a pressure transducer and a pressure gauge. At the top of the test section there was a water plenum (box with 0.71 m length, 0.63 m width and 0.61 m height) which was open to the atmosphere, so that air was removed from the flow. After removing the air bubbles the water returns via a downcomer pipe to the pump. Based on the principle of continuity, the water level in the header tank is kept constant when the system is running.

The test section consists of three pipe segments, two of them (the bottom and the top segments) are made from perspex and the other one from opaque PVC, all with an internal diameter of 100 mm. The perspex pipe segments were used for observing the air bubble behaviour using a high speed camera. The pressure wave signals were detected by the pressure transducers. The pressure oscillation data was recorded and analysed using a PC, an oscilloscope and a signal analyser. Data acquisition software called 'GLOBAL LAB®' was used to capture the pressure wave signals from the transducers with a sample rate frequency of 2000 Hz. In order to ensure reliable pressure signals, the transducer tapping holes were degassed after the test section is filled with water. Additionally, the four transducers were calibrated prior to use. They were put at the same height in the pipe and found to give reasonable consistent readings of the pulse amplitude on a cross section profile, as shown in Fig. 2.

The purpose of the bubble generator was to create an air–water two-phase flow that was as homogeneous as possible. It was important that there was uniformity in velocity distribution, turbulence intensity, void fraction and bubble size at the test section. Fig. 3 illustrates the design outline of the bubble generator. Pressurized air was supplied to four wing-shaped injectors installed in parallel across the passage at 25 mm pitch. As the figure indicates, the injectors had side walls made of perforated 1 mm thick brass sheet and the air formed tiny bubbles on the surfaces. In order to use different void fractions and distributions in the test, two designs of the bubble generators were used having 1600 and 160 holes of 0.75 and 0.5 mm diameter, respectively. The thickness of the injector profile reduces to 0 from 6 mm at the leading edge. The air supply system is also illustrated schematically in Fig. 1. Pressurized air from a low pressure air supply entered a pressure regulator and then its flowrate was controlled by a valve and measured using a rotameter. Air was supplied to the four injectors via independent, flexible, small diameter piping. As gravity can force the water into the air feed piping, a non-return valve was needed in the air supply line. In the event of

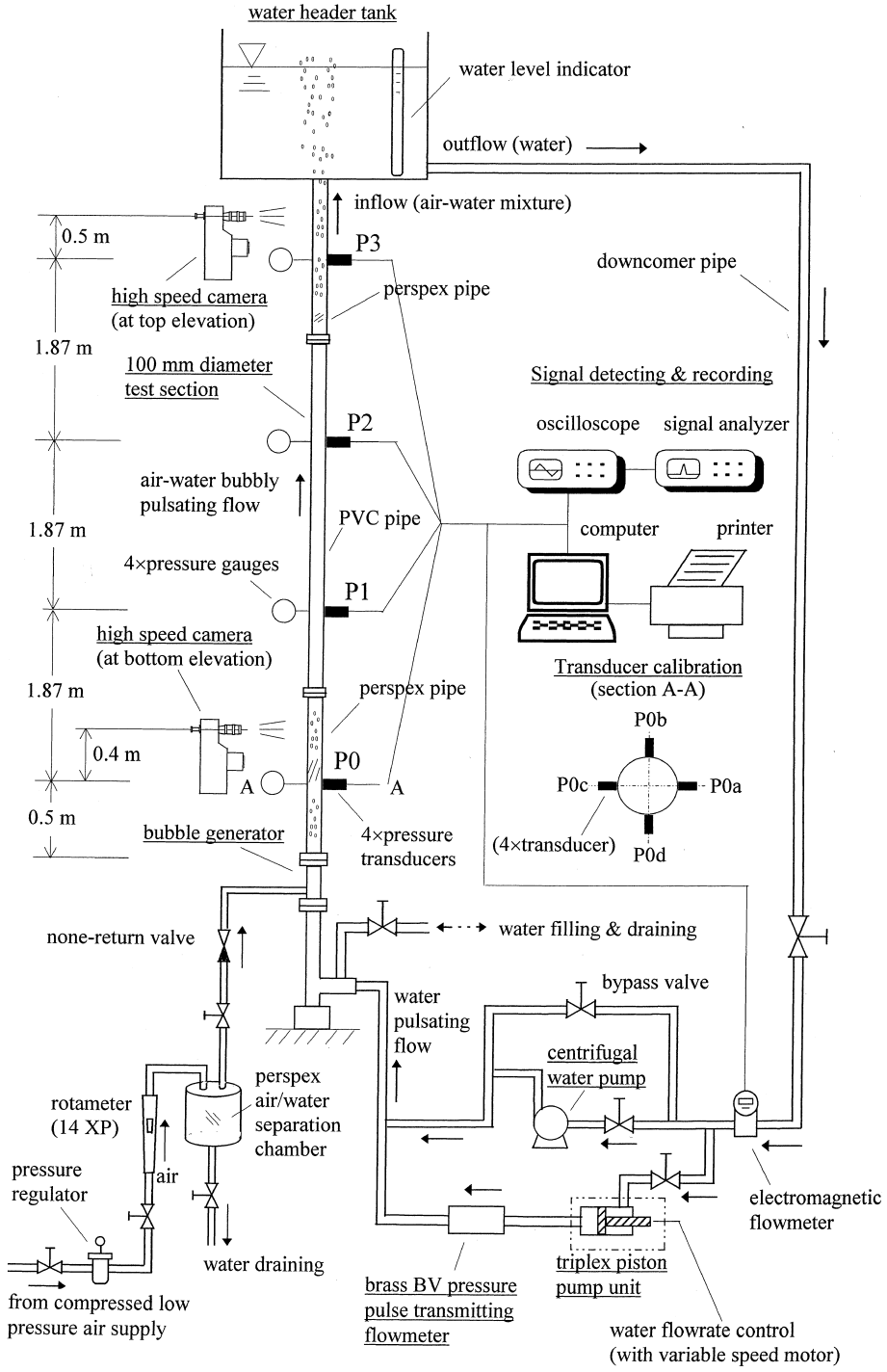

Fig. 1. Schematic of air–water bubbly flow rig for pressure wave transmission.

water dropping through this valve, a perspex separation chamber was used to accumulate and drain the water.

3. Pressure wave transmission measurements

Before the experimental results are described, two important parameters for the bubbly pipe flow, void fraction and homogeneous Reynolds number, are required to be defined. The term global air void fraction can be defined in integral form as

$$\alpha = \frac{\int_{V_g} \mathrm{d}V}{\int_{V_g+V_L} \mathrm{d}V}, \tag{1}$$

where V_g and V_L are the volumes of air and water phase, respectively. In engineering applications it is customary to describe flow condition in terms of flowrate ratios. Eq. (1) can be approximated by a volume-average or bulk void fraction as

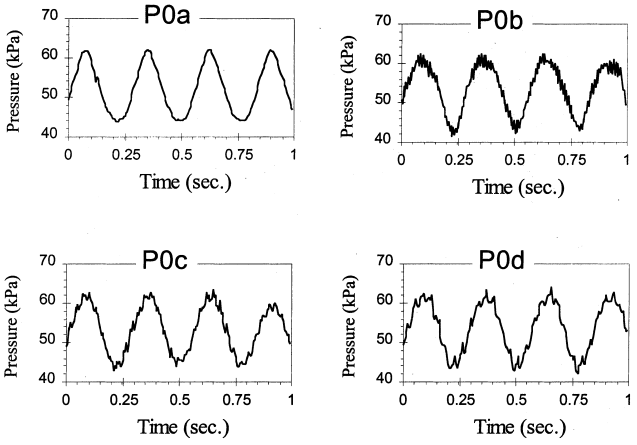

Fig. 2. Pressure pulse waveforms from the four transducers in a pipe cross sectional profile for $f=3.6$ Hz and $\alpha=6.7\%$.

$$\alpha=\frac{\int_{Q_g} dQ}{\int_{Q_g+Q_L} dQ}=\frac{Q_g}{Q_g+Q_L}, \tag{2}$$

where Q_g and Q_L are volume flowrates of the air and water, respectively. Eq. (2) was used to calculate the air void fractions from the tests and is independent of bubble size. The size of the individual bubbles is a function of the nature of the bubble generator.

The two-phase flow is usually considered as homogeneous flow in analyses. Thus suitable average properties can be determined and the mixture can be treated as a pseudofluid that obeys the usual equations of single phase flow (Beylich, 1994). From the homogeneous air–water bubbly flow model, defining the single phase fluid with density of the mixture and the viscosity of the continuous phase, the homogeneous Reynolds number for the bubbly flow in the test can be given as:

$$Re_h=\frac{\rho_m D V_m}{\mu_L}, \tag{3}$$

where D is the diameter of the test section, μ_L denotes the viscosity of water, the continuous phase, and ρ_m is mean density of the mixture, which is defined as

$$\rho_m=\alpha\rho_g+(1-\alpha)\rho_L, \tag{4}$$

where ρ_g and ρ_l are densities of air and water, respectively. V_m in Eq. (3) is the superficial velocity or total flux (j) for the mixture which is noted as

$$V_m=j=j_L+j_g, \tag{5}$$

where j_L and j_g are the fluxes or superficial velocities for water and air phase, respectively, which are given as

$$j_L=\frac{4Q_L}{\pi D^2}, \quad j_g=\frac{4Q_g}{\pi D^2}. \tag{6}$$

Thus the homogeneous Reynolds number for the bubbly flow can be re-written from Eq. (3) as

$$Re_h=\frac{(j_L+j_g)D\left[\alpha\rho_g+(1-\alpha)\rho_L\right]}{\mu_L}. \tag{7}$$

Using Eqs. (2), (5) and (6), the superficial velocity for the mixture can be re-written as

$$V_m=4\left(\frac{1}{1-\alpha}\right)\frac{Q_L}{\pi D^2}=\left(\frac{1}{1-\alpha}\right)j_L. \tag{8}$$

So from Eq. (8), another form of Eq. (3) can be written as

$$\begin{aligned} Re_h&=4\left(\frac{\alpha}{1-\alpha}\rho_g+\rho_L\right)\frac{Q_L}{\pi\mu_L D}\\ &=\left(\frac{\alpha}{1-\alpha}\cdot\frac{\rho_g}{\rho_L}+1\right)Re_L \end{aligned} \tag{9}$$

because of $\rho_L\gg\rho_g$, $Re_h\approx Re_L$ and thus independent of air void within the void fraction range tested.Using the experimental facilities shown and described in Fig. 1, tests were done to detect pressure waves with different void fractions (up to 25%) and wave frequencies (between 4 and 12 Hz). Fig. 4 shows the pressure waveforms at the different measuring stations at a frequency of 9.6 Hz for air void fractions of 4% and 9.1%, respectively. The captured pressure signals shown in Fig. 4 are clear (noting the scale change on graphs), with some 'noise' which can be attributed to random interfacial pressure fluctuations, a characteristic phenomenon of bubbly two phase flow, as reviewed earlier.

The pressure wave decay along the pulsating flow is of vital importance to know how much pressure wave remains for detection downstream. The experimental amplitude reduction shown in Fig. 4 between successive stations is seen to increase with increasing void fraction at the same frequency. The wave amplitude, A, is simply defined as

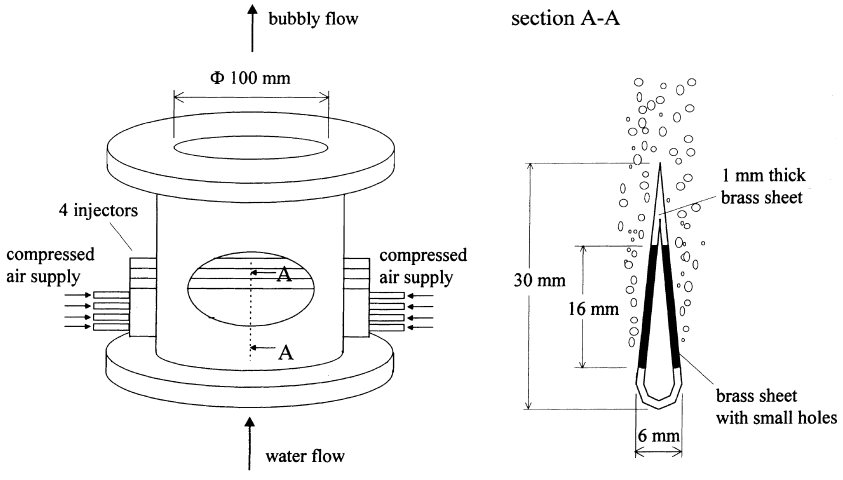

Fig. 3. Outline of the bubble generator.

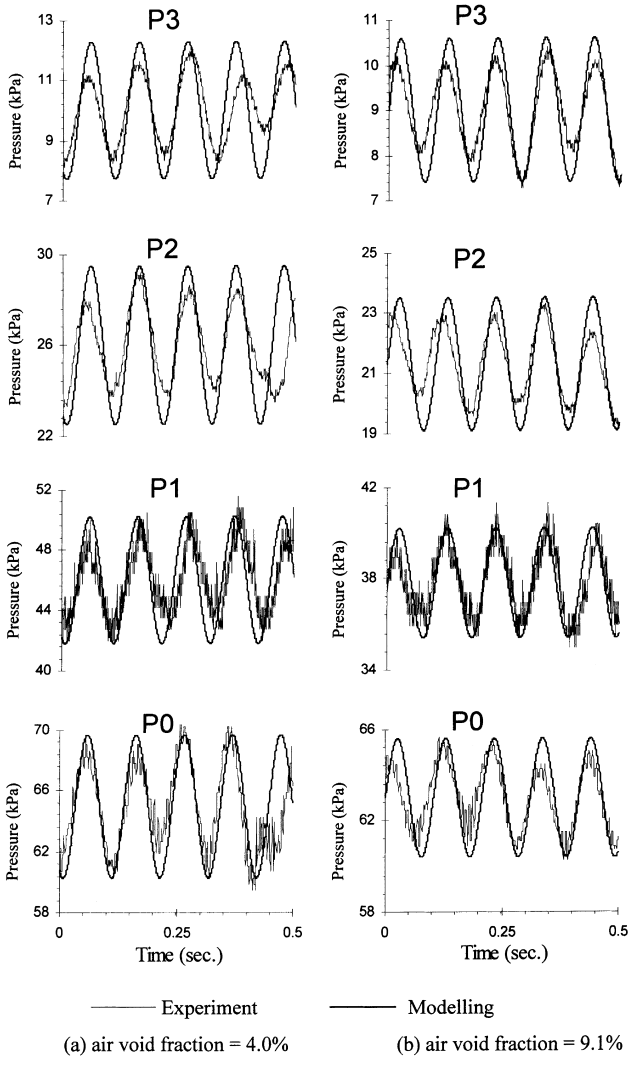

Fig. 4. Pressure waveforms in air–water bubbly flow for wave frequency 9.6 Hz. Thin lines: experiment; thick lines: modelling.

$$A = P_{\max} - P_{\min}. \tag{10}$$

This is found from statistical data of the global characteristics of the wave transmission, where $P_{\max}$ and $P_{\min}$ are maximum and minimum transient pressures, respectively. A simple parameter, the pressure wave remaining (PWR), was used to describe a relative amplitude for the wave decay. The PWR was defined as

$$\mathrm{PWR}(\%) = \frac{A}{A_0}100, \tag{11}$$

where A and A_0 are downstream and upstream pressure wave amplitude, respectively, and the upstream measuring station is specified as P0 (reading of the bottom transducer). Fig. 5 shows how the PWR decreases with the elevation above the bottom transducer for different air void fractions. It can be seen that increasing the air void fraction increases the pressure wave decay at a given wave frequency.

Fig. 6 shows how the pressure wave decays with height for different frequencies at a given void fraction of 9.1%, with all the water flow passing through the BV flowmeter. It can be seen that, over the range tested, increasing frequency increases wave attenuation (or reduces the wave remaining) at each measuring station. It should be noted that the higher frequency

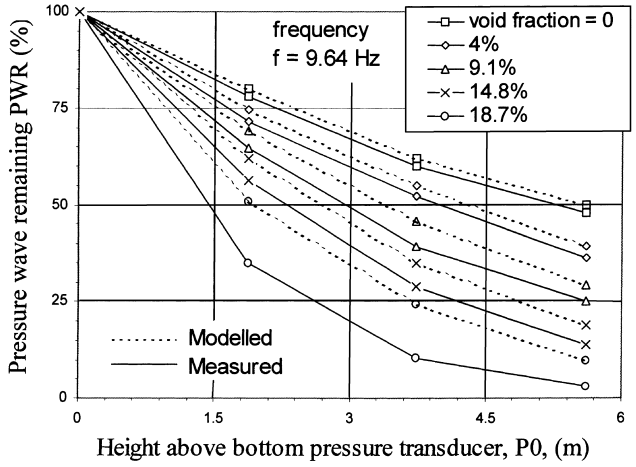

Fig. 5. Effect of elevation on pressure wave decay for different air void fraction.

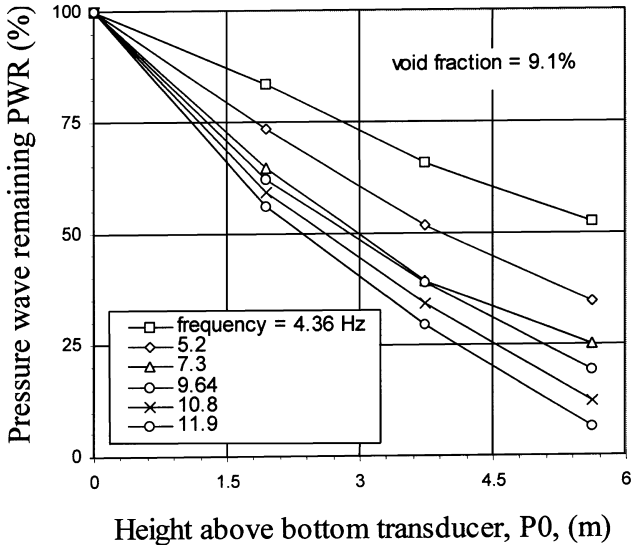

Fig. 6. Pressure wave decay along the mixed flow for different wave frequency.

waves also had higher amplitudes, this being a characteristic of the BV flowmeter as the water flowrate increased. Furthermore a linear relationship of wave frequency and water flowrate was verified, as shown in Fig. 7, when all the water flow was passing through the BV flowmeter. The water flowrate and wave frequency were measured using the electromagnetic flowmeter and signal analyzer, respectively.

4. Behaviour of air bubbles in a pressure wave

The effect of bubble size and distribution on the pressure waves in the air–water bubble flow was studied using high speed photography. A high speed motion picture camera, operating at approximately 4000 frames/s, was used. The camera was located at the top and bottom elevations (Fig. 1). Pictures were taken in selected runs with different air void fraction and wave frequency. Many sequential photographs were analyzed in detail by a film projecting the photographs to a large screen, both at various projection speeds and frame by

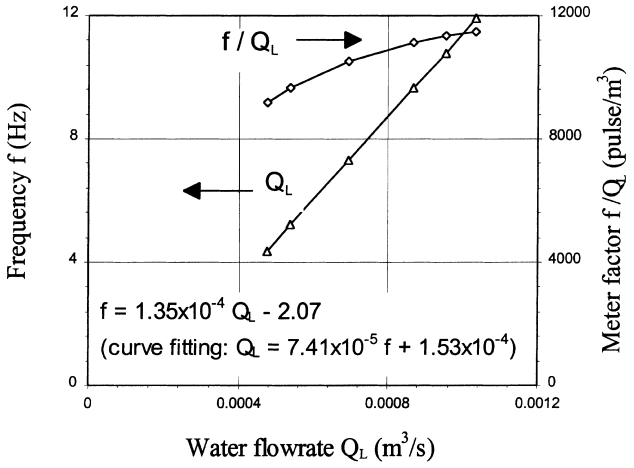

Fig. 7. Flowmeter calibration.

frame, to decide: (1) the initial state (no pressure waves) of the bubbly flow in the test section; (2) the gross effect of the pressure wave on the bubbly mixture; (3) the effect of the pressure wave on individual air bubbles.

Fig. 8 shows sample photographs of the air bubbles passing the bottom and top elevations (Fig. 1), for $\alpha = 4\%$ and $f = 9.64$ Hz. It can be seen that the shapes and distribution of the air bubbles are variable along the flow. For the initial state (no pressure waves) of the air–water bubbly mixture, studying the films to determine bubble size distribution showed that, for any given run within $\alpha < 20\%$, the bubbles were of approximately uniform size and that there was essentially no change in average bubble size even though the void fraction was varied up to 20%. If we neglect the shape change of the bubbles, for the case of Fig. 8, the bubble radius is approximately 3 mm. It was noted that with the bubble rise velocity remained constant, with an increase in the air flowrate resulting in an increase in the void fraction with more bubbles were formed in the flow. When void fraction exceeded about 20%, the chances of two bubbles colliding and coalescing greatly increased, such that the average bubble size increased until individual bubbles became comparable in size with the pipe diameter.

Another observation was that there were insignificant fluctuations in the average void fraction with time at a given axial location in the pipe. Over the range of void fractions used as $4\% < \alpha < 20\%$, the bubble density was almost uniform. This means that the bubble generator worked well and produced homogeneous bubbles with only small voidage fluctuation. The overall pressure wave in the bubbly mixture was followed by observing the changes in oscillation frequency or velocity of the mixture (note the frequency is proportional to the water flowrate when all the water went through the flowmeter) as the wave passed a given axial location in the pipe.

One general conclusion reached from viewing the films in detail was that the visible effects of the pressure wave on the occurred simultaneously over the cross section of the pipe. For example, observing the advancement of the wave front through the mixture frame by frame showed that as a bubble near the axis of the pipe started to compress, all the other bubbles in the perspex segment having the same axial position started to compress simultaneously. The effect of the pressure wave on the individual bubbles was found to be strongly dependent on the amplitude of the wave and to a lesser extent on the void fraction. Using the BV flowmeter to generate the pressure wave, increasing water flowrate also caused growth of both wave amplitude and frequency. Thus the effect of a pressure wave on individual bubbles cannot be distinguished from any possible effect of flowrate, but the latter is not expected to be significant.

For the waves and void fractions used, the bubbles were seen to be oscillating as a result of their initial compression by the wave. In general, the bubbles remained intact. At low void fractions, if the amplitude of the oscillations was fairly large, the bubbles often became badly distorted, with their horizontal diameter much larger than the vertical diameter. When initially compressed, some of the larger bubbles were distorted into a dished shape, the bottoms of the bubbles having been pushed up through the centers of the bubbles. Although a single fluctuation period for the bubbles was difficult to define, nevertheless the order of magnitude of the bubble fluctuation frequencies as measured from the motion pictures were the same as the frequencies of the recorded pressure fluctuations in the captured signals.

5. CFD modelling and comparison with experiments

There are several commercial CFD codes in use, and the majority have some capability for multi-phase flow modelling, each with its own particular set of features (Freitas, 1995). In this work the CFD code FLUENT (Fluent, 1996) was used. Both the Eulerian multiphase and the time dependent models are required to perform calculations of the pressure wave decay. The modelled flow field in the CFD simulation is an upward air–water bubbly flow, as shown in Fig. 1. The geometry of the flow domain is simple: a vertical pipe and its appended large plenum which relates to the water header tank. To sim-

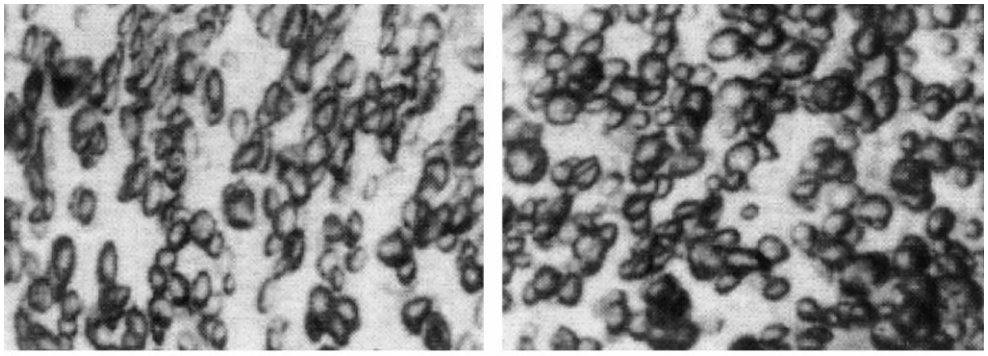

(a) Passing the bottom elevation (b) Passing the top elevation

Fig. 8. Photographs of the air bubbles in pulsating flow.

plify the problem, the outflow from the water header tank is neglected. This will have negligible effect on the accuracy of the solution as the size of the outflow duct is very small compared with the area of the water in the header tank. Moreover, the outflow position is remote from the inflow position connected to the test section and it does not affect the flow conditions of the upward flow in the test section.

To further simplify the geometry of the modelled domain to reduce computer effort, the appended plenum was treated as a cylinder with the same axis to the pipe. Obviously changing shape of the large plenum from cube to cylinder has a little effect on the flow in the test section. Thus the modelled domain has a cylindrical geometry enabling a cylindrical polar co-ordinate system to be used. Assuming the mixture flow is axisymmetric, a two-dimensional solution can be used. The centerline of the pipe and cylinder is represented by a set of boundary cells along the 'left' vertical line of the domain ($j=1$), in which the cells are set as symmetry cells, defined as a wall without shear. Therefore the geometry of the modelled domain with a length of pipe and cylinder was simulated using a Cartesian grid of I cells along the elevation by J cells wide along the radius as geometric grids. The heights of the pipe and cylinder were treated as the same as in the experiments. Hence, the mixture flow was modelled as a two-dimensional grid formed from 250 by 70 grid nodes in the I and J directions, respectively. Finer grid spacing was used in the junction region of the pipe and cylinder, where steep gradients of the dependent variables were expected.

Boundary conditions were specified as following: a no slip condition was used on the wall of the pipe and cylinder; a symmetry condition was applied on the center line; the inflow boundary condition was utilised as a Pressure INLET boundary condition I1, which was composed from a time-dependent harmonic pressure profile, based on the measured data from the test. In FLUENT, this inflow pressure INLET boundary is required to be input as total pressures. Clearly the outflow boundary for the domain is a free surface of the fluid. However, in the conditions of a test, the level of the free surface is constant due to continuity. Thus the outflow boundary can also be specified as a Pressure INLET Boundary condition I2, and the static pressure is required to be input. It was assumed that the I2 pressure could be defined as a constant at ambient pressure, and that the pressure wave signal decays completely in the I2 boundary. It is also important to note that in FLUENT the default gravitational acceleration is zero. For the current case of upward flow, the gravity force must be included and defined in magnitude and direction as the gravity vector.

To reduce the significant computational effort of solving the complicated problem of the bubble flow, solving techniques are required in calculations. For the first solution attempt it is customary to start with simple approximations and work up to the final form of the bubbly pulsating flow. An initial guess for the flow field and volume fractions is required for the mixture flow calculation. For the unsteady flow calculation required for this system, a steady-state flow solution is also necessary prior to the time dependent model being applied.

For this calculation, a grid of 17,500 nodes was used for the flow field and the computation was performed on a supercomputer. Each run required several hours of CPU time. For different flow conditions of air void fraction and pressure wave frequency, different CFD modelling results were obtained. Fig. 4 shows the modelled wave forms at the four measuring stations, for void fraction $\alpha=4$ and 9.1% respectively and a pulsation frequency of 9.64 Hz. The modelled harmonic pressure of P0 was imposed from the measured data of P0, and it was used as a time-dependent pressure profile of the inflow boundary condition in the CFD modelling.

The two comparisons which were made between experimental wave amplitude results and CFD predictions show a marked difference. From Fig. 4, the CFD predictions for the two void fractions can be seen to be in reasonable agreement with the measurements, but there is discrepancy between the measurements and predictions of the pressure pulse waveforms in particular the amplitude at P2 and P3. It is important to note that the observed and recorded waveforms not only depend on the gross flow conditions of wave frequency and void fraction, but also on many other factors, e.g., interfacial pressure fluctuations between the air and water phases, interaction of the pressure transducer with the different numbers and sizes of bubbles in its sensitive area, non-axisymmetric bubble number and different size distributions. The air phase in the mixture, the flow is susceptible to compressibility effects. The pressure fluctuations will be associated with the air volume expanding and contracting including inertial effects of the radially accelerating liquid. Interfacial effects (bubble vapour and air diffusion) and non-spherical bubbles are factors which affect the waveform but which the FLUENT Eulerian multiphase model cannot take into account.

In an attempt to know the differences between the measured wave amplitudes and CFD predicted results in tested range of void fraction (0–18.7%) within the bubble flow regime, CFD modellings for each case were also conducted. Fig. 5 shows the modeled and measured PWR along the bubbly flow with a wave frequency of 9.64 Hz for void fractions between 0% and 18.7%. Comparing the modelled results, it can be seen that increasing the void fraction produces a decrease of the predicted pressure wave amplitude at a given frequency and that the predictions from FLUENT gave reasonable agreement with measurement of the wave decay up to void fraction 14.8%. There is however disagreement between the measured and simulated results in the higher void fraction of 18.7%. It is probable that interfacial fluid exchange and non-axisymmetric bubble number distributions, not accounted for in the computations, became more important at higher void fractions.

6. Conclusions

Experiments and simulations have been conducted in order to investigate pressure wave attenuation along an upward flowing air–water bubbly flow. It is shown from the results of both experiments and simulations that the wave decay mainly depends on distance travelled, wave frequency and air void fraction. It was found that increasing void fraction results in the reduction of the detected wave amplitude at each measuring station. The experimental work has also verified that the pressure wave, produced by a BV fluidic pressure pulse transmitting flowmeter, propagates along the upward bubbly flow with a frequency proportional to the water flowrate, and that sufficient signal remains for remote flow measurement in the bubbly flow.

High speed photographs of the experiments show some of the effects of the pressure wave on the mixture and individual bubbles, providing an understanding of energy losses and bubble behaviour during the wave passing the mixture flow. Within the bubble flow regime of $\alpha \leqslant 20\%$ in the test, the average bubble size did not vary with void fraction when using a specially designed bubble generator in the test.

It has been shown that CFD modelling can give a reasonable realistic prediction of pressure wave attenuation in upward air–water bubbly flow. Using its Eulerian multiphase and time dependent models, predictions from FLUENT gave reasonable agreement with measurements in the range of wave frequencies between 4 and 12 Hz, air void fractions between 0% and 14.8% and the homogeneous Reynolds numbers up to

1.2×10^4. There were, however, substantial differences between the measured pressure wave amplitudes and CFD predictions at higher void fractions.

References

Akselrod, A.F. 1993. Pressure and Void Fraction Pulsations in Two-Phase Flow. Fluid Engineering Division Publications (FED) Gas–Liquid Flows – 1993, vol. 165. ASME, New York, pp. 187–190.

Beck, S.B.M., Boucher, R.F., 1993. Sheffield University Network Analysis Software (SUNAS), Department of Mechanical and Process Engineering, University of Sheffield, UK.

Beck, S.B.M., Haider, H., Boucher, R.F., 1995. Transmission line modelling of simulated drill strings undergoing water-hammer. Journal of Mechanical Engineering Science (Proceedings of The Institution of Mechanical Engineers) 209 (C6), 419–427.

Bertodano, M.L.D., Lahey, R.T., Jones, O.C., 1994. Development of a k–ε model for bubbly two-phase flow. Journal of Fluids Engineering 116, 128–134.

Beylich, A.E., 1995. Pressure waves in bubbly liquid. In: Morioka, S., Van Wijngaarden, L. (Eds.), Proceedings of the IUTAM Symposium on Waves in Liquid/Gas and Liquid/Vapour Two-Phase Systems 1994. Kluwer Academic Publishers, The Netherlands.

Boucher, R.F., Beck, S.B.M., Wang, H., 1996. A fluidic flowmetering device for remote measurement. Journal of Process Mechanical Engineering (Proceedings of the Institution of Mechanical Engineers) 210 (E2), 93–100.

Chung, N., Lin, W., Pei, B., Hsu, Y., 1992. A model for sound velocity in a two-phase air–water bubbly flow. Nuclear Technology 99, 80–89.

Commander, K.W., Prosperetti, A., 1989. Linear pressure waves in bubbly liquids – comparison between theory and experiments. Journal of the Acoustical Society of America 85 (2), 732–746.

Fluent, 1996. Fluent User's Guide, Version 4.4, 30th July, New Hampshire.

Freitas, C.J., 1995. Perspective: selected benchmarks from commercial CFD codes. Journal of Fluids Engineering (Transactions of the ASME) 117, 208–218.

Hsieh, D.Y., Plesset, M.S., 1961. On the propagation of sound in a liquid containing gas bubbles. The Physics of Fluids 4, 970–975.

Kameda, M., Matsumoto, Y., 1996. Shock waves in a liquid containing small gas bubbles. Physics of Fluids 8 (2), 322–335.

Kameda, M., Shimaura, N., Higashino, F., Matsumoto, Y., 1998. Shock waves in a uniform bubbly flow. Physics of Fluids 10 (10), 2661–2668.

Kuznestov, V.V., Nakoryakov, V.E., Pokusaev, B.G., Shreiber, I.R., 1978. Propagation of perturbations in a gas–liquid mixture. Part 1. Journal of Fluid Mechanics 85, 85–96.

Kytomaa, H.K., Brennen, C.E., 1991. Small amplitude kinematic wave propagation in two-component media. International Journal of Multiphase Flow 17 (1), 13–26.

Leutheusser, H.J. 1978. Experimental studies of two-phase air–water flows. In: Proceedings of the Dynamic Flow Conference, New York, pp. 397–405.

Lisseter, P.E., Fowler, A.C., 1992. Bubbly flow – I. A simplified model and II. Modelling void fraction waves. International Journal of Multiphase Flow 18, 195–215.

Liu, T.J., Bankoff, S.G., 1993. Structure of air–water bubble flow in a vertical pipe: I – liquid mean velocity and turbulence measurements. International Journal of Heat and Mass Transfer 36 (4), 1049–1060.

Miksis, M.J., Ting, L., 1992. Wave propagation in a bubbly liquid at small volume fraction. Chemical Engineering Communications 118, 59–73.

Nakoryakov, V.E., Kuznetsov, V.V., Dontsov, V.E., Markov, P.G., 1990. Pressure waves of moderate intensity in liquid with gas bubbles. International Journal of Multiphase Flow 16 (5), 741–749.

Nigmatulin, R.I., 1982. Mathematical modelling of bubbly liquid motion and hydrodynamical effects in wave propagation phenomenon. Applied Scientific Research 38, 267–289.

Pauchon, C., Banerjee, A., 1988. Interphase momentum interaction effects in the averaged multifield model. Part II: kinematic waves and interfacial drag in bubble flow. International Journal of Multiphase Flow 14, 253–264.

Prosperetti, A., Kim, D.H., 1988. Pressure Waves in Bubbly Liquids at Small Gas Volume Fractions. Fluids Engineering Division Publication, vol. 72. ASME, pp. 19–27.

Revankar, S.T., Ishii, M., 1992. Local interfacial area measurement in bubbly flow. International Journal of Heat and Mass Transfer 35 (4), 913–925.

Ruggle, A.E., 1988. An investigation of the propagation of pressure perturbations in bubbly air/water flows. Journal of Heat Transfer (Transactions of the ASME) 110, 494–499.

Serizawa, A., Kataoka, I., Michiyoshi, I., 1975. Turbulence structure of air–water bubbly flow. International Journal of Multiphase Flow 2 (3), 221–259.

Silberman, E., 1957. Sound velocity and attenuation in bubbly mixtures measured in standing wave tubes. Journal of the Acoustical Society of American 29 (8), 925–933.

Theofanous, T.G., Sullivan, J., 1982. Turbulence in two-phase flows. Journal of Fluid Mechanics 116, 343–362.

Thorley, A.R.D., 1991. Fluid Transients in Pipeline Systems, D. & L. George, Herts, England.

Van Wijngaarden, L., 1972. One-dimensional flow of liquids containing small gas bubbles. Annual Review of Fluid Mechanics 4, 369–396.

Van Wijngaarden, L., 1995. Evolving solitons in bubbly flows. Acta Applicandae Mathematicae 39 (1-3), 507–516.

Vreenegoor, A.J.N., Geurst, J.A., 1993. Two-phase bubble flow through vertical tube: void-fraction distribution and velocity profiles. Physica A 192, 410–442.

Wallis, G.B., 1969. One-Dimensional Two-Phase Flow. Mcgraw-Hill, New York.

Wang, H., Priestman, G.H., Beck, S.B.M., Boucher, R.F., 1996. Development of fluidic flowmeters for monitoring crude oil production. Flow Measurement and Instrumentation 7 (2), 91–98.

Wang, H., Beck, S.B.M., Priestman, G.H., Boucher, R.F., 1997. Fluidic pressure pulse transmitting flowmeter. Transactions of the Institution of Chemical Engineers. Part A. Chemical Engineering Research and Design 75 (A4), 381–391.

Wang, H., Priestman, G.H., Beck, S.B.M., Boucher, R.F., 1998. A remote measuring flowmeter for petroleum and other industrial applications. Measurement Science and Technology 9 (5), 779–789.

Wang, H., Priestman, G.H., Beck, S.B.M., Boucher, R.F., 1999. Pressure wave attenuation in an air pipe flow. Journal of Mechanical Engineering Science (Proceedings of the Institution of Mechanical Engineers), to be published.

Watanabe, M., Prosperetti, A., 1994. Shock waves in dilute bubbly liquids. Journal of Fluid Mechanics 274, 349–381.

Wylie, E.B., Streeter, V.L., 1985. Fluid Transients. FEB Press, Ann Arbor, Michigan 48106.